This document is the accepted manuscript version of the following article:
Gischkat, T., Schachtler, D., Steger, F., Balogh-Michels, Z., Vetsch, B., Strüning, T., … Neels, A. (2023). Low-temperature ion beam sputtered optical coatings. Applied Optics, 62(7), B195-B201. https://doi.org/10.1364/AO.480089

Low Temperature Ion Beam Sputtered Optical Coatings

TH. Gischkat,[1*] D. Schachtler,[1] F. Steger,[1] Z. Balogh-Michels,[1] B. Vetsch,[2] T. Strüning,[3] J. Birkhölzer,[3] M. Michler,[3] Ch. Mühlig,[4,5] S. Schwinde,[5] M. Trost,[5] S. Schröder,[5] A. Borzi,[6] and A. Neels[6]

[1]*RhySearch, Werdenbergstr. 4, 9471 Buchs, Switzerland*
[2]*ThermodynamX Straubstrasse 11, 7323 Vilters-Wangs, Switzerland*
[3]*OST - University of Applied Sciences Buchs, Werdenbergstr. 4, 9471 Buchs, Switzerland*
[4]*Leibniz-IPHT, Albert-Einstein-Str. 9, 07745 Jena, Germany*
[5]*Fraunhofer IOF, Albert-Einstein-Str. 7, 07745 Jena, Germany*
[6]*EMPA, Ueberlandstrasse 129, 8600 Dübendorf, Switzerland*
**thomas.gischkat@iof.fraunhofer.de*

Abstract: In thin film deposition processes the lower limit of the deposition temperature is determined by the used coating technology and the duration of the coating process and usually higher than room temperature. Hence, processing of thermal sensitive materials and the adjustability of thin film morphology are limited. In consequence, for factual low temperature deposition processes an active cooling of the substrate is required. The effect of low substrate temperature on thin film properties during the ion beam sputtering was investigated. The SiO_2 and Ta_2O_5 films grown at 0°C show a trend of lower optical losses and higher LIDT compared to 100°C.

1. Introduction

Optical systems are an integral part in a wide range of applications, e.g., consumer products, industrial tools, aeronautics as well as scientific equipment. Thereby almost all optical components are functionalized by an optical coating, which defines the transmission, reflection and the optical losses of the optical system [1]. Conversely, the requirements on the optical component define the optical thin film design as well as the thin film properties (e.g., refractive index, extinction coefficient, and laser damage resistance). Both are strongly related to the applied materials and the used deposition technique [2-4].

It is well known that in case of physical vapor deposition processes the thin film properties depend on coating technology and the deposition parameters including the substrate temperature [5]. Especially the thin film growth and morphology depend strongly on the energy of the adatoms and the substrate temperature T_s in relation to the melting temperature T_m [6]. Primarily, the coating technology defines the energy of the evaporated atoms and in consequence the surface mobility of the adatoms. Whereby, the energy can vary between < 0.1 eV and > 100 eV for e-beam and sputtering processes, respectively. In order to increase the film quality in case of low energy deposition processes the substrate temperature has to be high as possible. For example, the coating temperature of e-beam evaporation processes is typically above 200°C [7-9]. Nevertheless dense, non-porous and smooth films are only achievable using sputter processes where the kinetic energy of the adatoms is high enough even at room temperature [9]. Though, due to the transferred energy of the energetic atoms in plasma processes the substrate temperature rises up to almost 100°C depending on process duration and parameters. In case of temperature sensitive substrates and processes, e.g., polymers or cemented components the applicable design are limited in accordance to the total thickness (i.e. deposition time) or cooling down breaks have to be introduced. In consequence, low temperature processes are required to keep the substrate temperature well below 100°C. Furthermore, in case of deposition materials with low melting points the accessible T_s/T_m ratio is limited compared to materials with higher melting points.

Here, we present an active cooled substrate holder that is implemented in an ion beam sputter tool for thin film deposition at substrate temperatures down to 0°C. Using this, we investigated the thin film properties of ion beam sputtered SiO_2 and Ta_2O_5 for a substrate temperature of 0°C and compare the results to standard substrate temperatures of about 100°C.

2. Methods

2.1 Thin film deposition system

A Veeco Spector 1.5 Dual Ion Beam Sputter (DIBS) tool was used for the thin film deposition. The tool is equipped with a 16 cm and a 12 cm three-grid end-hall RF ion beam source for sputtering and for assisting purposes, respectively. Pump down of the chamber is realized by means of a cryo-pump system. The base pressure was below $1x10^{-7}$ Torr. In order to avoid particle contamination of the substrates, the sputter tool is installed in a cleanroom environment (ISO 5–7).

Together with ThermodynamX, a customized cooling system with a cooling capacity of 200 W at approx. -20°C/35°C evaporating/condensing temperature was developed. The water-cooled refrigeration cycle consists of a refrigeration compressor, a water-cooled condenser, the vacuum chamber feed through for feed and return lines of the evaporator and several additional measures to vary the target temperature and cooling capacity. In Figure 1 the integration of the feed and the return lines as well as the active cooled substrate holder assembly is shown.

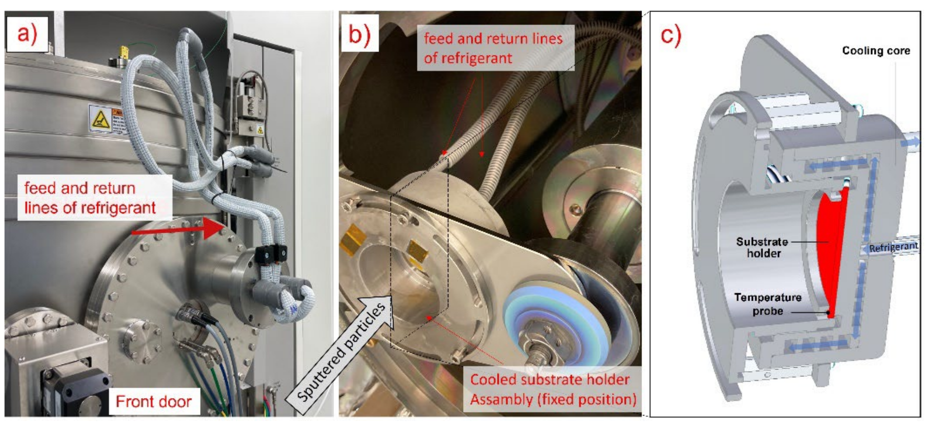

Fig. 1. Front view of the Veeco Dual Ion Beam Sputter (DIBS) tool (a) and inside view on the cooled substrate holder with fixed position (b) as well as a cross section view of the substrate holder assembly (c).

The evaporator (fig.1 b) is a vacuum-sealed 2 inch substrate holder assembly inside of the chamber to cool actively the substrates during the deposition process. As refrigerant, non-flammable R513A was used. A Kapton insulated thermocouple type K was used to measure the surface temperature of the substrate by contact. Additionally an IR-thermal imaging camera (FLIR T650sc) was used. In case of the IR-camera a ZnS-Viewport was installed on the back of the coating chamber. A customized software was developed that allows the controlling and graphical rendering of the substrate temperature as well as refrigerant temperature. In order to avoid incorrect measurements due to less thermal conduct of the thermoelement we used the temperature of the refrigerant for controlling purposes.

The 2 inch substrate holder (fused silica substrate, thickness 2 mm) is clamped in the substrate holder assembly (fig. 1 c). The deposition induced thermal energy is transferred from the substrate to the refrigerant due to the direct thermal conduct. In order to provide best thermal conductivity, the substrate holder was conducted to the cooling holder using a UHV vacuum grease (Braycote Micronic 803). The substrates were subsequently glued using conductive silver paint to guarantee best thermal contact. After deposition the conductive silver paint was removed and the substrates were carefully cleaned by acetone and isopropanol.

2.2 Sample preparation

For our investigations, we chose the widely applied optical thin film materials SiO_2 and Ta_2O_5. Sputtering was realized using a ceramic and a metallic target, respectively. The ion incidence angle was 45°, the polar emission angle was 30° with a resulting sputter angle of about 105° [10]. We deposited single layers with a physical thickness of about 270 nm for both coating materials. In case of laser damage testing, a Ta_2O_5 single layer with an optical thickness of about 3 QW @ 355 nm for normal incidence was grown. Besides single layers, a high reflectance mirror (Sub - [L H]17 2L – air @ 638 nm, angle of incidence aoi = 0°) for a central wavelength of 638 nm for normal incidence was deposited. The estimated reflection R_{theor} was > 99.99%.

As substrates, Ø25.4x2.0 mm^2 fused silica and 10x10 mm^2 Si-wafer were used. Different polishing grades with rms roughness values of 3 nm, 0.4 nm and < 0.1 nm were used. By the fact that particles and other residuals can have a dramatic effect on the thin film properties all samples were cleaned precisely prior the deposition process [11]. In order to investigate the effect of low temperature ion beam sputtering on the thin film properties, the substrate temperature during the deposition was set to 0° as well as at 100°C for comparison purposes. The deposition temperature of 100°C was set and controlled via the standard coating tool software and equipment (thermolement type K, thermo controller EUROTHERM 2408 and quartz lamp heater).

After thin film deposition, all coated samples were subsequently thermal treated for 24 hours at 400°C under air condition in a conventional furnace.

2.3 Thin film characterization

Different methods were used to characterize the deposited thin films. The optical properties were determined by means of a PerkinElmer Lambda 1050 equipped with a GPOB (General-Purpose Optical Bench) by measuring the transmission spectra. The spectra were subsequently fitted using FTG FilmStar in order to determine the dispersion and extinction of the single layers as well as the thickness and the deposition rate, respectively. Laser induced deflection (LID) at 532 nm was performed to determine the absorption losses in the single layers [12]. The reflection and total optical losses of the mirror coating were investigated by means of a cavity ring down at 638 nm and an angle of incidence of about 0°.

The laser damage resistance in ns-regime was investigated at 355 nm and 532 nm using a laser damage test bench equipped with a Q-switched LITRON diode pumped Nd:YAG light source. The repetition rate was 100 Hz with a pulse duration of the beam of about 10 ns. In accordance with ISO norm 21254 the Gaussian beam profile's effective beam diameter was above 200 µm (1/e2). A S-on-1 measurement strategy [13] was applied with S = 1000. The centered test area was 20 mm in diameter and divided into a hexagonal test matrix with equidistant measurement sites. According to the beam diameter and the ISO norm, each test site's distances were larger than 5 times the beam diameter. The measurement was performed in filtered air and at room temperature. The detection of damage events was realized by a scattering detector that was placed in front of the test sample. In order to verify the detected damage morphologies, visual inspection by means of differential interference contrast DIC-microscopy was performed.

Additional X-ray measurement methods (XRD, GISAXS) were used to investigate the crystallinity of the grown films.

3. Results and discussion

Figure 2 shows for a standard deposition process the temperature as a function of the process time inside of the coating chamber measured by means of a thermoelement. Without pre-heating the temperature inside of the chamber stabilizes after 30 minutes pump down time at almost 18 °C. After starting the ion beam sources and the thin film deposition, the temperature starts immediately to increase continuously. Approximately 30 min after switching on the ion beam sources (total process time 60 min) a temperature of about ~40 °C is reached. As it can be observed that the temperature saturates almost 180 min after starting the ion beam sources (total process time 210 min) at a temperature of about 80 °C. Only a slight further increase up to 82°C is observable until the process is finished. Thus, pre-heating of the tool before starting the deposition process is recommended in order to avoid temperature related inhomogeneities in the thin film growth and properties due to the substrate temperature shift.

3.1 Active cooling

After installation of the active cooling system, we measured the temperature of the substrate in vacuum using a FLIR thermal imaging camera as well as with a thermoelement. The results are shown in Figure 3. As it can be seen (Fig 3a) the measured temperature on the surface is between -1.3°C (point 6) and -2.9°C (points 4 and 5) revealing a very good temperature homogeneity of +/- 1 K over a 2-inch wafer. Turning on the ion beam sources leads to an increase of the substrate surface temperature. In saturation state the difference between the measured temperature of the substrate and the refrigerant was 10 K. This offset was considered and integrated in the active cooling software for setting the parameters.

The temperature on the substrate (blue) surface as well as of the refrigerant (red) during a coating test process is shown in Figure 3b measured by means of the thermoelement. The temperature setting in the software is also included (black). Before starting the process, we set the temperature in the software to 10°C. Due to the integrated offset mentioned above the system cooled down to 0°C. By the fact that no additional thermal energy is transferred to the system both the refrigerant and substrate had the same temperature in the saturation state. After starting the process, the substrate temperature increases due to the transferred energy and reach a maximum of approximately 10°C (time = 13500 s). Reducing the setpoint (substrate) to a target of 5°C, the temperature of the refrigerator decreases and in consequence the substrate temperature too. With maximum cooling (temperature setting to -25°C) the refrigerant reaches -10°C and the substrate saturates at almost 0°C. The temperature gap between substrate and refrigerator saturates at about 10 K.

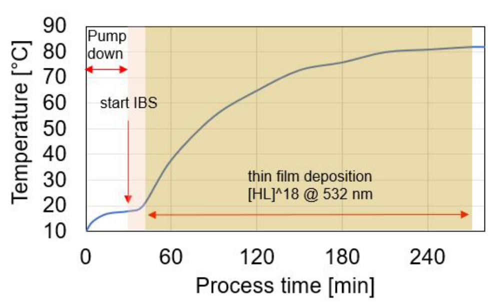

Fig. 2. Temperature inside of the chamber as a function of time for a standard coating process without pre-heating of the chamber.

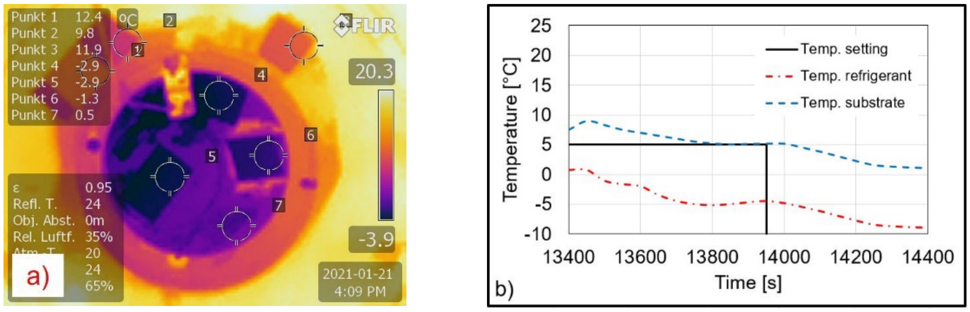

Fig. 3. Temperature distribution of the cooled substrate holder (a) and temperature of the substrate as well the refrigerant during process (b).

3.2 Single layer

Figure 4 shows the spectral transmission of the thermally treated (24 h @ 400°C) SiO_2 and Ta_2O_5 single layers grown at a temperature of 0°C and 100°C (in the following referred to as *low* and *high temperature*, respectively). FTG Filmstar was used to fit the transmission spectra in order to estimate the refractive index as function of the wavelength. As it can also be concluded from the transmission spectra, the refractive index is nearly independent of the temperature within the error limits. For example, in case of Ta_2O_5 the refractive index *n* is about 2.12 at a wavelength of 532 nm. In case of SiO_2 the estimated refractive index is 1.48 at 532 nm wavelength. The growth rates of the single layers are for SiO2 and Ta_2O_5 and low temperature approximately 0.46 nm/s and in case of high temperature slightly higher (1%). The determined absorption losses at 532 nm are 11 +/-2 ppm and 30 +/-4 ppm for SiO_2 and Ta_2O_5, respectively. Similar to the refractive index, the absorption losses were temperature independent within the measurement accuracy.

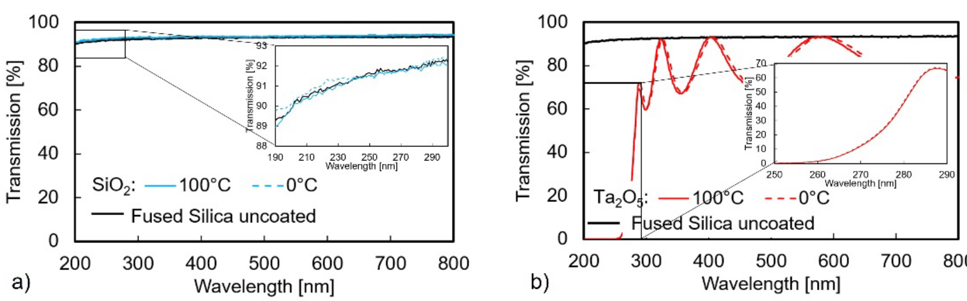

Fig. 4. Transmission spectra of (a) SiO2- and (b) Ta2O5 single layer for a deposition temperature of 0°C and 100°C. The insets give a zoom in the UV-region.

In order to investigate the influence of substrate temperature on the laser induced damage behavior, Ta_2O_5 single layers (3QW at 355 nm, angle of incidence = 0°) were laser damage tested at 355 nm wavelength using ns-pulses. In Figure 5, typical defect morphologies of laser induced damages are shown. As it can be seen there are no remarkable differences indicating similar defect mechanism for both substrate temperatures.

Figure 6 shows the results of the laser damage testing for the low and high temperature deposition. The damage probabilities (black and red dots) were calculated using the cumulative data reduction technique [14]. In accordance with ISO 21254, a linear fit was applied (black and red dashed line). The corresponding characteristic damage curves for 0%- and 50%-LIDT are shown in Figure 6b. In contrast to the results before, the laser induced damage behavior depends clearly on the substrate temperature during the deposition process. For the same laser induced damage probability (Figure 6a) the required fluence is for low temperature deposition (black curve) significantly higher than for the deposition at high temperature (red curves). In more detail, the damage onset is for the high temperature at a fluence of 0.5 J/cm^2 and for the low temperature to 1 J/cm^2. A damage probability of almost 100% is reached for a laser beam fluence of about 1.5 J/cm^2 and 2.0 J/cm^2 for high and low temperatures, respectively.

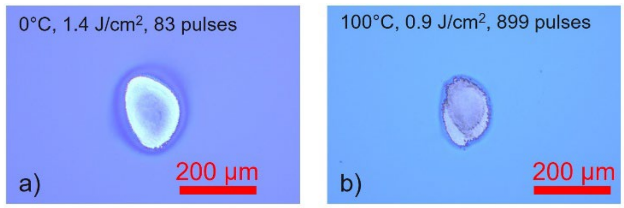

Fig. 5 microscopic pictures of typical damage sites of the Ta2O5 single layers grown at (a) 0°C and (b) 100°C.

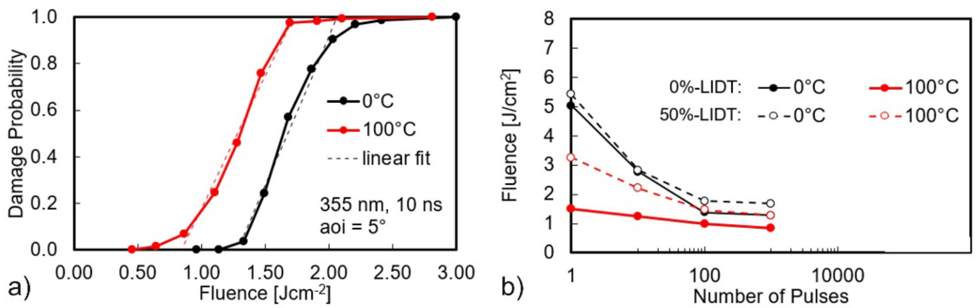

Fig. 6. Damage probability as a function of the laser fluence (a) and characteristic damage curve for 0%-and 50%-LIDT (b) for the 3QW (355 nm, 0°) Ta2O5 grown at 0°C (black curves) and 100°C (red curves).

As it can be seen in Figure 6b the characteristic damage curves taken at 0%- and 50%-LIDT show a different behavior for both substrate temperatures and defect levels indicating different fatigue and degradation effects. For low temperature deposition (black curves) the relative change in LIDT from 1 to 1000 pulses is higher compared to the high substrate temperature (red curves). Furthermore, in case of high substrate temperature the fatigue and degradation effect depend on the damage level that is not the case for the low temperature.

In order to investigate the thin film structure GIXRD measurements were performed. The measurement results for SiO_2 and Ta_2O_5 single layers are shown in Fig 7. The 2 Theta scans appear in all cases almost x-ray amorphous. As it can be seen for both materials no differences for low and standard deposition temperature are observable. Additional investigations by means of GISAXS technique showed that the deposited films are completely x-ray amorphous at any order of distances.

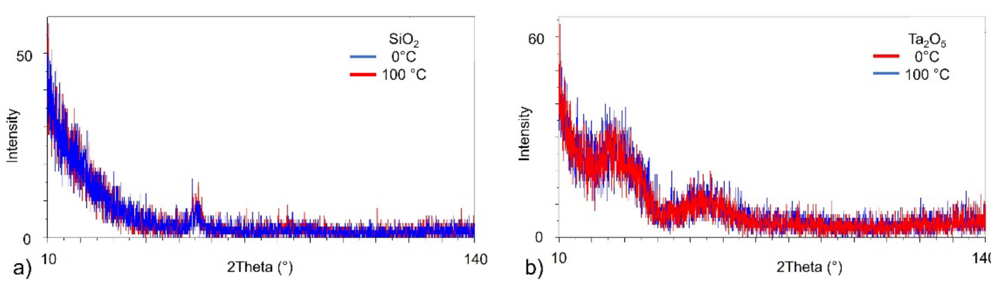

Fig. 7. 2Theta XRD-measurements on (a) SiO2 single layers and (b)Ta2O5 single layers.

3.3 High reflectance mirror

The deposited high reflectance mirrors were designed for a wavelength of 638 nm and an angle of incidence of 0°. Using the determined optical properties of the deposited SiO_2 and Ta_2O_5 single layers the theoretical reflection was above 99.99%. In Figure 8, the transmission spectra for low and high temperature are depicted in linear and logarithmic scale. Due to uncertainties in the deposition rate, the minimum in transmission (i.e. maximum in reflectance) are slightly shifted compared to the design wavelength of 638 nm (gray line in fig 8b). The expected maximum in reflection is at 622 nm for the low and at 645 nm for the high coating temperature, respectively. However, at 638 nm the residual transmission is for the deposition at 0°C about (2.7 +/- 0.3) x 10^{-3} % and for 100°C about (1.9 +/- 0.3) x 10^{-3} %. The optical losses were measured for normal incidence (angle of incidence = 0°) by means of cavity ring down using a 638 nm laser beam source. The estimated total losses (1- R) were 560 ppm in case of high temperature and 125 ppm for low temperature deposition.

Laser damage testing of the high reflectance mirrors were done at a wavelength of 532 nm. Therefore, in order to match the wavelength, the HR was tilted during the irradiation to an angle of incidence of 45° with respect to the laser beam. Figure 9 shows the results of the laser damage testing for the low and high temperature. As it can be seen similar to the laser beam irradiation of Ta_2O_5, the damage probabilities depend strongly on the coating temperature. The required fluences for the same degree of laser induced damage are remarkable higher for the deposition at low temperature compared to the high temperature. For high temperatures, a damage on set is observed at a fluence of 4 J/cm^2 and a 100% damage probability was measured for a fluence of 24 J/cm^2. In case of low temperature, the on set is drastically increased to 15 J/cm^2. Accordingly, a fluence of 39 J/cm^2 is required for a damage probability of 100%.

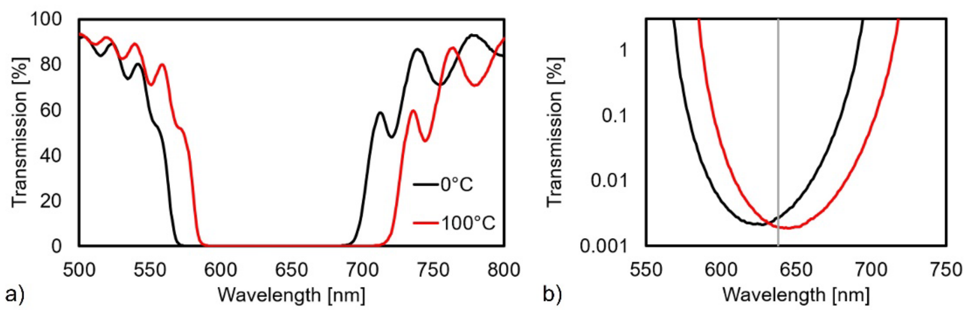

Fig. 8. Transmission spectra of the HR-mirror grown at 0°C (black curve) and 100°C (red curve).

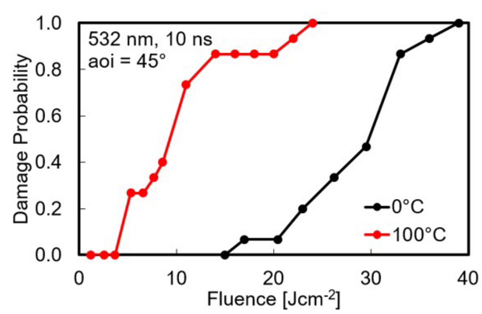

Fig. 9. Damage probability of laser beam irradiated HR-mirrors at a wavelength of 532 nm.

3.4 Discussion

Regarding the most relevant optical properties for optical thin film designing like refractive index, dispersion and extinction the deposition temperature has no significant influence within the error limits. In case of more sensitive optical properties like total optical losses and laser induced damage threshold an influence of the substrate temperature during the thin film growth can be observed. By the fact that the deposited layers seem to be x-ray amorphous at any order of distance this effect is not related to structural effects in a first assumption.

It is known from investigations on thin carbon films prepared by ion beam sputtering and UV laser vaporization at temperatures between 77 K and 573 K that the sp2/sp3 binding ratio depends strongly on the deposition temperature and substrate thermal diffusivity [15]. In the first instance the energy of the particles created by laser as well as ion beam technique is sufficient high enough to exceed the sp2 → sp3 barrier. In case of film growth at elevated temperatures and low thermal diffusivity, the energy of the adatoms keeps high enough to relax from sp3 to the sp2, subsequently. With decreasing temperature of the substrate (i.e. room temperature and below) the energy of the adatoms is removed immediately and a thermal quenching effect occurs. In consequence the fraction of relaxing particles to sp2 decreases and the film becomes more diamond like. We assume that in case of the deposition of SiO_2 and Ta_2O_5 at a substrate temperature of 0°C a similar effect occurs and influences the optical properties like total losses and laser induced damage behavior.

Using the laser damage testing results for the Ta_2O_5 single layers in Figure 6, the differences in fluence ($\Delta F = F_{100°C} - F_{0°C}$) that are required for a given damage probability as well as the difference in the characteristic damage curves are calculated and depicted in figure 10. As it can be seen in all cases, the differences in fluence decrease indicating different laser induced relaxation of the thin film. We assume that compared to high temperature deposition in case of low temperature different metastable states are created and partially relax with increasing deposited laser energy (i.e. fluence and no. of pulses).

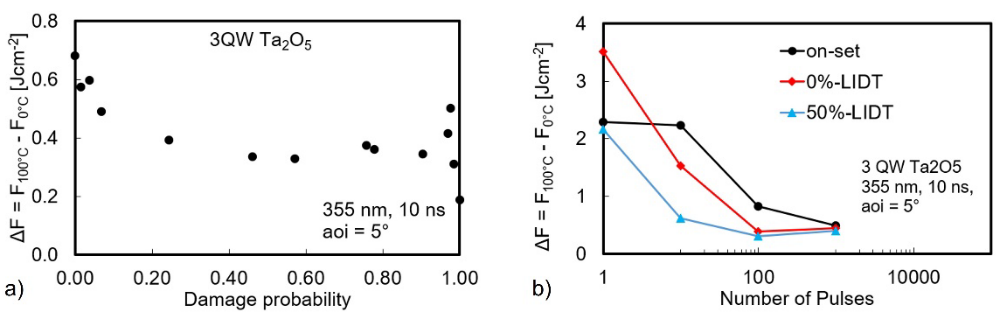

Fig. 10. Differences in fluence for 100°C and 0°C to the generate the same degree of laser induced damage (a) and difference of the characteristic damage curves for 100°C and 0°C (b).

4. Conclusion

In this work, we presented an active substrate cooling system implemented on our dual ion beam sputter tool. Thus, we were able to deposit thin films at substrate temperatures well controlled below the technology related saturation chamber temperature. Using this, we investigated the influence of low temperature (i.e., 0°C) on optical properties compared to standard deposition temperature of 100°C. The refractive index, dispersion, and extinction coefficient were not significant influenced by the decreased substrate temperature during thin film growth. In case of total optical losses and the laser induced damage threshold an influence of the growth temperature was found. We observed a trend to lower optical losses and higher LIDT in case of lower substrate temperature compared to the standard coating at elevated temperature (100°C).

With respect to the analysis by means of x-ray techniques the difference in the losses and LIDT cannot explained by a structural effect as the films appear amorphous at any order of distance. In accordance with findings in the literature, we assume that a thermal quenching effect occurs at low temperatures that leads to different binding character. In order to verify the findings more research is required and will be investigated in further experiments (e.g. using Raman spectroscopy).

Acknowledgments. We would like to thank Innosuisse, the government of St. Gallen Switzerland and the Principality of Liechtenstein for their financial support and funding of RhySearch.

Disclosures. The authors declare no conflicts of interest.

References

1. H. A. Macleod, “Thin-Film Optical Filters (4th ed.),” CRC Press (2010).
2. D. Ristau, “Laser-Induced Damage in Optical Materials,” CRC Press (2015).
3. N. Kaiser and H. K. Pulker, “Optical Interference Coatings,” Springer Berlin, Heidelberg (2003).
4. O. Stenzel, “Optical Coatings,” Springer Berlin, Heidelberg (2014).
5. D. M. Mattox, “Handbook of Physical Vapor Deposition (PVD) Processing (2^{nd} ed.),” Elsevier (2010).
6. J. A. Thornton, "Structure-Zone Models of Thin Films", Proc. SPIE 0821, Modeling of Optical Thin Films (1988).
7. C.-C. Jaing, et al, “Effects of Ion Assistance and Substrate Temperature on Optical Characteristics and Microstructure of MgF_2 Films Formed by Electron Beam Evaporation,” Jpn. J. Appl. Phys. 45 5027 (2006).
8. D. Pjević, et al., “Influence of substrate temperature and annealing on structural and optical properties of TiO2 films deposited by reactive e-beam evaporation,” Thin Solid Films, Volume 591, Part B (2015).
9. M. Cevro and G. Carter, “Ion beam sputtering and dual ion beam sputtering of titanium oxide films,” J. Phys. D: Appl. Phys. 28 (1995).
10. C. Bundesmann and H. Neumann, “Tutorial: The Systematics of Ion Beam Sputtering for Deposition of Thin Films with Tailored Properties” (Invited, Editor's Pick), J. Appl. Phys., 124 231102 (2018), DOI: 10.1063/1.5054046.
11. Th. Gischkat, et al., “Substrate Cleaning Processes and Their Influence on the Laser Resistance of Anti-Reflective Coatings,” Appl. Sci. 10(23) (2020).
12. S. Bublitz, C. Mühlig, “Absolute Absorption Measurements in Optical Coatings by Laser Induced Deflection,” Coatings 9(8) (2019). doi.org/10.3390/coatings9080473
13. J. Shao, “Laser-Induced Damage in Optical Materials,” Ristau, D., Ed.; CRC Press: Boca Raton, FL, USA, Chapter 6, pp. 167–169 (2014).
14. L. Jensen, M. Mrohs, M. Gyamfi, H. Mädebach, D. Ristau, “Higher certainty of the laser-induced damage threshold test with a redistributing data treatment,” Rev. Sci. Instrum. 86, 103106-1–103106-6 (2015).
15. J. J. Cuomo, et al., "Sputter deposition of dense diamond-like carbon films at low temperature," Appl. Phys. Lett. 58, 466-468 (1991) https://doi.org/10.1063/1.104609.